complexes: Pd (1.0) < Ni (1.7) < Pt (10.2), determined in methanol.[29a] Qualitative studies of the acidities of group 9 complexes give the following order of decreasing acidities: HRhL₄ > HCoL₄ > HIrL₄ (L = CO, PF₃, respectively).[34] Recently, Morris and co-workers[35] reported increasing pK_a values of *trans*-[MH(η^2-H₂)(PR₂CH₂CH₂PR₂)₂]⁺ (R = Ph, *p*-CF₃C₆H₄) complexes in the order Fe < Os < Ru. This latter example and that of **3** and **8** (Table I) are the first reported examples of a reversal between complexes of second- and third-row metals.

ΔH_{HM} **of Cp*₂M, Where M = Ru, Os.** The basicities of the Cp*₂M complexes, **9** and **10**, also increase on going down the column from Ru (ΔH_{HM} = −19.0 kcal mol⁻¹) to Os (ΔH_{HM} = −26.6 kcal mol⁻¹). In terms of equilibrium constants for protonation, **10** is 4 × 10⁵ times more basic than **9** assuming $\Delta S^\ominus$ is the same for both reactions. Qualitative studies of the basicities of Cp₂Fe and Cp₂Ru reported previously[29b,32] indicate that the Ru complex is more basic than the Fe complex. This suggests that Cp*₂Fe will also be less basic than Cp*₂Ru (**9**) although we were unable to obtain a ΔH_{HM} value for Cp*₂Fe. In contrast to those of complexes **1**, **2**, and **7** above, the electrochemical potentials (vs SCE in CH₂Cl₂)[33] of **9** ($E_{1/2}$ = 0.55 V) and **10** ($E_{1/2}$ = 0.46 V) decrease as one goes down the group.

Basicities of Organonitrogen Complexes, ΔH_{HN}. The wide range of ΔH_{HM} values from −19.0 kcal mol⁻¹ for complex **4** to −38.7 kcal mol⁻¹ for complex **6** demonstrates that substantial changes in metal basicity occur upon changing the metal and/or the chelate ligand. A comparable range of ΔH_{HN} values was obtained for the six organonitrogen bases in Table I. The variation from the weakly basic 3-bromopyridine to the strongly basic tetramethylguanidine is 17.6 kcal mol⁻¹. The ΔH_{HN} values for these organonitrogen bases correlate linearly (r = 0.997) with their pK_a values[36] in water (eq 10). A similar correlation (eq 11) of

$$-\Delta H_{HN} = 1.64 \ pK_a + 21.0 \ ; \ \text{in kcal mol}^{-1} \tag{10}$$

$$-\Delta H_{HP} = 1.82 \ pK_a + 16.3; \ \text{in kcal mol}^{-1} \tag{11}$$

the heats of protonation (ΔH_{HP}) of a series of phosphines with their pK_a values was previously reported.[10,17] It is evident, that while the correlations in eq 10 and 11 are similar, they are distinctly different for these two different families of compounds. Arnett and Scorrano[37] previously reported correlations of the heats of protonation in FSO₃H with pK_a values for various organic bases; these correlations were also different for different families of compounds.

(34) (a) Vidal, J. L.; Walker, W. E. *Inorg. Chem.* **1981**, *20*, 249. (b) Kruck, T.; Lang, W.; Derner, N.; Stadler, M. *Chem. Ber.* **1968**, *101*, 3816.
(35) Reported in the: *Abstracts of Papers*, 4th Chemical Congress of North America and 202nd National Meeting of the American Chemical Society, New York; American Chemical Society: Washington, DC, 1991; Inorganic Division, No. 380.
(36) Perrin, D. D. *Dissociation Constants of Organic Bases in Aqueous Solution*; Butterworths: London, 1972.
(37) Arnett, E. M.; Scorrano, G. *Adv. Phys. Org. Chem.* **1976**, *13*, 83.

Contribution from the Department of Chemistry,
The University of North Carolina, Chapel Hill, North Carolina 27599-3290

Redox and Spectral Properties of the Four-Electron Oxidant *trans*-[Ru(tpy)(O)₂(H₂O)](ClO₄)₂

S. Ajao Adeyemi, Angelos Dovletoglou, Ana R. Guadalupe, and Thomas J. Meyer*

The complex *trans*-[Ru(tpy)(O)₂(H₂O)](ClO₄)₂ (**1**) (tpy is 2,2′:6′,2″-terpyridine) has been prepared and characterized by UV–visible, FTIR, resonance Raman, and ¹H NMR spectroscopies and earlier by X-ray crystallography. Its redox properties were investigated by electrochemical techniques over the pH range 0–9 in water. The couples Ru(VI/IV), Ru(IV/III), and Ru(III/II) appear and are pH dependent. At pH = 1.0, $E_{1/2}$ values for *trans*-[Ru^VI(tpy)(O)₂(H₂O)]²⁺/[Ru^IV(tpy)(O)(H₂O)₂]²⁺, [Ru^IV(tpy)(O)(H₂O)₂]²⁺/[Ru^III(tpy)(H₂O)₃]³⁺, and [Ru^III(tpy)(H₂O)₃]³⁺/[Ru^II(tpy)(H₂O)₃]²⁺ are 1.27, 1.11, and 0.71 V vs NHE. Plots of $E_{1/2}$ vs pH are revealing in defining regions of stability for the various oxidation states and in defining the pK_a values of their aqua and hydroxo forms. An intense band appears in the infrared spectrum of **1** at 841 cm⁻¹ in KBr, and an intense Raman band, at 834 cm⁻¹ in the solid state. These have been assigned to ν_{as}(O=Ru=O) and ν_{sym}(O=Ru=O), respectively. From the results of an X-ray crystallographic study, reported previously, the average Ru=O bond length is 1.661 Å and the O=Ru=O angle of the *trans*-dioxo group is 171.3° with the bending occurring away from the tpy ligand. Addition of **1** to CH₃CN led to *trans*-[Ru^VI(tpy)(O)₂(CH₃CN)]²⁺ (k_1 = 4.9 ● 0.2 s⁻¹, 19.5 °C), and addition of H₂O to the CH₃CN solution, to the reappearance of **1** (k_{-1} = 35.3 ● 0.1 M⁻¹ s⁻¹). The value of the equilibrium constant, K (=k_1/k_{-1}) = 0.15 ± 0.01 M, was determined independently from ¹H NMR studies in D₂O/CD₃CN mixtures. Comparisons with redox potentials for related couples and a thermodynamic analysis based on related ruthenium and structurally equivalent complexes of osmium reveal a number of features that may bear on the reactivity of **1** in solution.

Introduction

Oxo and dioxo complexes of the higher oxidation states of Ru(IV), Ru(V), and Ru(VI), have proven to be useful stoichiometric and catalytic oxidants.[1–4] An extensive chemistry of *trans*-dioxo complexes of Ru(VI) and Os(VI) is emerging based on porphyrins,[4] macrocycles,[5] polypyridyl complexes,[6,7] and py-

(1) (a) Nugent, W. A.; Mayer, J. M. *Metal–Ligand Multiple Bonds*; John Wiley: New York, 1988. (b) Meyer, T. J. In *Metal Oxo Complexes and Oxygen Activation*; Martell, A. E., Ed.; Plenum: New York, 1988; pp 33–47. (c) Holm, R. H. *Chem. Rev.* **1987**, *87*, 1401. (d) Gulliver, D. J.; Levason, W. *Coord. Chem. Rev.* **1982**, *46*, 1. (e) Sheldon, R. A.; Kochi, J. K. *Metal-Catalyzed Oxidations of Organic Compounds*; Academic: New York, 1981.

(2) (a) Dovletoglou, A.; Adeyemi, S. A.; Lynn, M. H.; Hodgson, D. J.; Meyer, T. J. *J. Am. Chem. Soc.* **1990**, *112*, 8989. (b) Dobson, J. C.; Meyer, T. J. *Inorg. Chem.* **1989**, *28*, 2013. (c) Seok, W. K.; Meyer, T. J. *J. Am. Chem. Soc.* **1988**, *110*, 7358. (d) Roecker, L.; Meyer, T. J. *J. Am. Chem. Soc.* **1987**, *109*, 746; **1986**, *108*, 4066. (e) Gilbert, J. A.; Roecker, L.; Meyer, T. J. *Inorg. Chem.* **1987**, *26*, 1126. (f) Thompson, M. S.; Meyer, T. J. *J. Am. Chem. Soc.* **1982**, *104*, 4106, 5070. (g) Moyer, B. A.; Thompson, M. S.; Meyer, T. J. *J. Am. Chem. Soc.* **1980**, *102*, 2310.

ridyl–carboxylato complexes.[8] Recently Che and co-workers,[9] and Griffith and co-workers[10] have been able to isolate Ru(V)–oxo complexes and have determined their structures by X-ray crystallography.

In the d^2 electronic configuration of M(VI) (M = Ru, Os), there is considerable stabilization of the *trans*-dioxo isomer compared to the cis isomer. The origin of the effect lies in electronic interactions between the $d\pi$ orbitals of the metal with $p\pi$ orbitals of the oxygen atoms, which lead to oxo–metal–oxo π bonding.[11] The loss of this stabilization in the cis isomer, e.g., in comparing *cis*- and *trans*-$[Ru^{VI}(bpy)_2(O)_2]^{2+}$, leads to a destabilization of Ru(VI) with an associated enhancement in the thermodynamic oxidizing strength of the cis isomer. In addition, the *cis*-dioxo geometry offers, at least in principle, some of the mechanistic advantages of the oxidants MO_4 (M = Ru, Os)[12] in having adjacent oxo groups which could open new oxidation pathways. One possibility would be the utilization of the *cis*-dioxo structure to achieve a four-electron oxidation at a single site.

Even given the implied advantages of the cis isomer as an oxidant compared to the trans, cis isomers of Ru(VI) are difficult to prepare in a stable form. For example, it is possible to generate *cis*-$[Ru^{VI}(bpy)_2(O)_2]^{2+}$ from *cis*-$[Ru^{II}(bpy)_2(H_2O)_2]^{2+}$ by electrochemical or chemical oxidation, but it is unstable with respect to chelate ring opening and *trans*-dioxo formation.[6a]

$$cis\text{-}[Ru(bpy)_2(O)_2]^{2+} + 2H_2O \rightarrow$$
$$trans,cis\text{-}[Ru(bpy)(O)_2(OH)_2]^{2+} + bpyH^+ + H^+$$
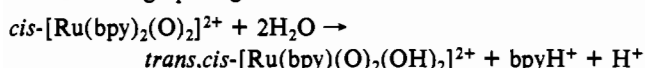
Strategies have been developed which attempt to stabilize the cis isomers but they have met with limited success.[13] In this

manuscript, we describe a strategy designed to achieve cis reactivity through an isomer that is initially trans. The strategy was based on preparing a *trans*-dioxo complex having a cis-aqua ligand. A *cis*-dioxo-like reactivity could exist for this structure if (1) the redox chemistry occurs in a stepwise manner, Ru(VI) → Ru(IV), Ru(IV) → Ru(II), (2) the strong electronic preference for the position of the oxo group is lost upon reduction of Ru^{VI} (d^2) to Ru^{IV} (d^4), and (3) a pathway exists by which the remaining oxo group in Ru(IV) can be transferred between sites within the coordination sphere
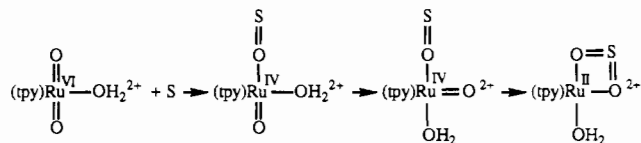
(S is the reducing agent). If it occurs, this transformation could provide a mechanistic basis for a *cis*-dioxo reactivity. Part of this work has appeared in a preliminary communication.[2a]

Experimental Section

Materials. Deuterium oxide (99.9% D, Aldrich Gold Label), 99.8% acetonitrile-d_3 (99.6% D), 2,4-pentanedione, 3-chloro-2,4-pentanedione, $Na_2C_2O_4$, and $RuCl_3·3H_2O$, were purchased from Aldrich Chemical Co. The ligand 2,2′:6′,2″-terpyridine, solutions of 0.5 N Ce(IV) in 6 N perchloric acid, and $(NH_4)_2Ce(NO_3)_6$ were purchased from G. F. Smith Chemicals. Spectrograde acetonitrile (Burdick & Jackson) was used as received. All other common reagents were ACS grade and were used without additional purification. Distilled water was purified additionally by passage through a Nanopure (Barnstead) water purification system.

Elemental Analysis. Microanalyses were conducted by Galbraith Laboratories, Knoxville, TN.

Preparations. [Ru(tpy)Cl₃] was prepared as described previously.[14]

[Ru(tpy)(acac)Cl]·1.5H₂O. A 0.50-g quantity of (tpy)RuCl₃ (1.13 mmol) was suspended in 150 mL of methanol already deaerated with nitrogen gas. A 0.5-mL quantity of triethylamine was added to the reaction vessel. To this mixture was added a ~10% excess amount of 2,4-pentanedione (acetylacetone) (0.12 g, 1.24 mmol), and the mixture was heated at reflux for 2 h under N_2 to obtain a purple solution. The reaction solution was filtered hot, and 0.1 g of LiCl was added to the filtrate before its volume was reduced to 20 mL on a rotary evaporator. The final solution was left in a refrigerator overnight to obtain a dark solid. The solid was filtered and washed twice with a minimum volume of cold water. It was purified by Soxhlet extraction under nitrogen with methanol containing 0.1 g of LiCl. Yield: 40%. Anal. Calcd for $C_{20}H_{21}N_3O_{3.5}ClRu$: C, 48.44; H, 4.27; N, 8.47; Cl, 7.15. Found: C, 48.06; H, 4.16; N, 8.39; Cl, 7.84.

[Ru(tpy)(3-Cl-acac)Cl]·H₂O [(3-Cl-acac) = 3-Chloro-2,4-pentanedione]. This compound was prepared by following the procedure for the isolation of the acetylacetonato complex. The solid product was stored under nitrogen. Yield: 30%. Anal. Calcd for $C_{20}H_{19}N_3O_3Cl_2Ru$: C, 46.08; H, 3.67; N, 8.06; Cl, 13.60. Found: C, 46.19; H, 3.73; N, 8.10; Cl, 13.38.

[Ru(tpy)(acac)(OH₂)](PF₆). For this preparation 0.50 mmol of [Ru(tpy)(acac)Cl]·1.5H₂O was suspended in 50 mL of water already deaerated with nitrogen, and the mixture was heated at reflux under nitrogen for 30 min to form the maroon aqua complex. The solution was filtered and ~20 mL of an aqueous solution saturated in ammonium hexafluorophosphate was added. The volume was reduced to ~35 mL on a rotary evaporator. The dark brown precipitate that formed was filtered, washed twice with water, air dried, and dried in vacuo over P_2O_5. Yield: 70%. Anal. Calcd for $C_{20}H_{20}N_3O_3PF_6Ru$: C, 40.28; H, 3.38; N, 7.05. Found: C, 40.43; H, 3.49; N, 7.07.

[Ru(tpy)(3-Cl-acac)(OH₂)](PF₆)·H₂O. This salt was prepared by following the procedure for the isolation of the acetylacetonato complex. Yield: 70%. Anal. Calcd for $C_{20}H_{21}N_3O_4ClPF_6Ru$: C, 37.02; H, 3.26; N, 6.48; Cl, 5.46. Found: C, 36.95; H, 3.22; N, 6.59; Cl, 5.47.

[Ru(tpy)(C₂O₄)(H₂O)]·2H₂O. A 1.00-g (2.27-mmol) quantity of Ru(tpy)Cl₃ was suspended in 350 mL of a methanol–water (1:2) mixture already deaerated with nitrogen in a 500-mL three-necked round-bottom flask, and 1.0 mL of triethylamine (7.2 mmol) was added to the stirred suspension of Ru(tpy)Cl₃. A 0.45-g (3.36-mmol) quantity of $Na_2C_2O_4$ was dissolved in a minimum amount of water in an addition funnel

(3) (a) Leung, W. H.; Che, C. M. *J. Am. Chem. Soc.* **1989**, *111*, 8812. (b) Yam, V. W.-W.; Che, C. M.; Tang, W. T. *J. Chem. Soc., Chem. Commun.* **1988**, 100. (c) Che, C. M.; Lee, W. O. *J. Chem. Soc., Chem. Commun.* **1988**, 881. (d) Wong, K. Y.; Che, C. M.; Anson, F. C. *Inorg. Chem.* **1987**, *26*, 737.

(4) (a) Groves, J. T.; Ahn, K. H. *Inorg. Chem.* **1987**, *26*, 3831. (b) Groves, J. T.; Quinn, R. *J. Am. Chem. Soc.* **1985**, *107*, 5790. (c) Groves, J. T.; Quinn, R. *Inorg. Chem.* **1984**, *23*, 3844.

(5) (a) Che, C. M.; Tang, W. T.; Wong, W. T.; Lai, T. F. *J. Am. Chem. Soc.* **1989**, *111*, 9048. (b) Che, C. M.; Tang, W. T.; Lee, W. O.; Wong, W. T.; Lai, T. F. *J. Chem. Soc., Dalton Trans.* **1989**, 2011. (c) Che, C. M.; Tang, W. T.; Lam, M. H.-W.; Mak, T. C. W. *J. Chem. Soc., Dalton Trans.* **1988**, 2885.

(6) (a) Dobson, J. C.; Meyer, T. J. *Inorg. Chem.* **1988**, *27*, 3283. (b) Dobson, J. C.; Takeuchi, K. J.; Pipes, D. W.; Geselowitz, D. A.; Meyer, T. J. *Inorg. Chem.* **1986**, *25*, 2357. (c) Pipes, D. W.; Meyer, T. J. *Inorg. Chem.* **1986**, *25*, 4042; *J. Am. Chem. Soc.* **1984**, *106*, 7653.

(7) (a) Marmion, M. E.; Takeuchi, K. J. *J. Am. Chem. Soc.* **1988**, *110*, 1472; **1986**, *108*, 510; *J. Chem. Soc., Chem. Commun.* **1987**, 1396. (b) Bigham, W. S.; Shapley, P. A. *Inorg. Chem.* **1991**, *30*, 4093.

(8) (a) Griffith, W. P.; Jolliffe, J. M.; Ley, S. V.; Williams, D. J. *J. Chem. Soc., Chem. Commun.* **1990**, 1219. (b) El-Hendawy, A. M.; Griffith, W. P.; Taha, F. I.; Moussa, M. N. *J. Chem. Soc., Dalton Trans.* **1989**, 901. (c) Dengel, A. C.; El-Hendawy, A. M.; Griffith, W. P.; O'Mahoney, C. A.; Williams, D. J. *J. Chem. Soc., Dalton Trans.* **1990**, 737. (d) Perrier, S.; Lau, T. C.; Kochi, J. K. *Inorg. Chem.* **1990**, *29*, 4190.

(9) Che, C. M.; Yam, V. W.-W.; Mak, T. C. W. *J. Am. Chem. Soc.* **1990**, *112*, 2284.

(10) Dengel, A. C.; Griffith, W. P.; O'Mahoney, C. A.; Williams, D. J. *J. Chem. Soc., Chem. Commun.* **1989**, 1720.

(11) (a) Ballhausen, C. J.; Gray, H. B. *Inorg. Chem.* **1962**, *1*, 111. (b) Gray, H. B.; Hare, C. R. *Inorg. Chem.* **1962**, *1*, 363. (c) Griffith, W. P.; Wickins, T. D. *J. Am. Chem. Soc. A* **1968**, 400. (d) Atovmyan, L. O.; Porai-Koshits, M. A. *J. Struct. Chem. (Engl. Transl.)* **1969**, *10*, 740. (e) Mingos, D. M. P. *J. Organomet. Chem.* **1979**, *179*, C29. (f) Mayer, J. M. *Comments Inorg. Chem.* **1988**, *8*, 125.

(12) (a) Wai, J. S. M.; Marco, I.; Svendsen, J. S.; Finn, M. G.; Jacobsen, E. N.; Sharpless, K. B. *J. Am. Chem. Soc.* **1989**, *111*, 1123. (b) Jorgensen, K. A.; Hoffmann, R. J. *J. Am. Chem. Soc.* **1986**, *108*, 1867. (c) Carlsen, P. H. J.; Katsuki, T.; Martin, V. S.; Sharpless, K. B. *J. Org. Chem.* **1981**, *46*, 3936. (d) Hentges, S. G.; Sharpless, K. B. *J. Am. Chem. Soc.* **1980**, *102*, 4263. (e) Schroder, M.; Nielson, A. J.; Griffith, W. P. *J. Chem. Soc., Dalton Trans.* **1979**, 1607. For review: (f) Schroder, M. *Chem. Rev.* **1980**, *80*, 187. (g) Muller, P. In *The Chemistry of the Functional Groups: Ethers, Grown Ethers and Hydroxyl Groups*, Patai, S., Ed.; Wiley: Chichester, England. 1980; Vol 1, p 469. (h) Lee, D. G.; van den Engh, M. In *Oxidation in Organic Chemistry*, Trahanovsky, W. S., Ed.; Academic: New York, 1973; Vol 5, part B, p 177.

(13) (a) Che, C. M.; Leung, W. H. *J. Chem. Soc., Chem. Commun.* **1987**, 1376. (b) Bailey, C. L.; Drago, R. S. *J. Chem. Soc., Chem. Commun.* **1987**, 179. (c) Collin, J. P.; Sauvage, J. P. *Inorg. Chem.* **1986**, *25*, 135.

(14) Sullivan, B. P.; Calvert, J. M.; Meyer, T. J. *Inorg. Chem.* **1980**, *19*, 1404.

attached to the third arm of the reaction vessel. The sodium oxalate solution was added dropwise to the reaction mixture with stirring, and the reaction mixture was heated at reflux under nitrogen for $2^1/_2$ h. The resulting purple solution was filtered hot to remove any unreacted solid. The volume of the filtrate was reduced on a rotary evaporator to about 80 mL and the remaining sample left in the refrigerator overnight. The black solid that formed was filtered, washed twice with a minimum volume of cold water, and then dried in vacuo over P_2O_5. Yield: 60%. Anal. Calcd for $C_{17}H_{17}N_3O_7Ru$: C, 42.86; H, 3.60; N, 8.82. Found: C, 43.03; H, 3.46; N, 9.13.

***trans*-[Ru(tpy)(O)₂(H₂O)](ClO₄)₂·H₂O.** A 0.15-g (0.32-mmol) quantity of [Ru(tpy)(C₂O₄)(H₂O)]·2H₂O was suspended and stirred in 4 mL of a 2 M HClO₄ solution until it dissolved to give a deep red-maroon solution. This solution, which contained [Ru(tpy)(H₂O)₃]²⁺, was filtered, and the filtrate was added dropwise to a magnetically stirred solution containing a 20-fold excess of Ce(IV) (0.5 N Ce(IV) in 6 N HClO₄ or (NH₄)₂Ce(NO₃)₆ in 2 M HClO₄), which caused the solution to turn yellow. A yellow, microcrystalline solid appeared a few minutes after the addition of the oxalato complex was complete. The reaction mixture was stirred for 2 h and left to cool at 4 °C for ~4 h. The yellow solid that appeared was collected on a glass frit. If the yellow solid was found to be contaminated with a green compound at this point, it was purified by the slow addition of few drops of water. The pure yellow compound, which was dissolved in the water, was collected in 10 mL of 1 M HClO₄ containing 10% (NH₄)₂Ce(NO₃)₆. The washing was continued until the filtrate washings were no longer yellow. The microcrystalline, yellow solid that appeared in the 10% acidified Ce(IV) solution was filtered, washed twice with a minimum volume of ice-cold 0.1 M HClO₄ solution, air dried, and then dried in vacuo over P₂O₅ overnight. *Caution! Extra care was taken in the removal of the yellow solid sample from the frit. It was observed to explode with a red flame occasionally when the frit was scratched with a metal spatula.* Yield: 80%. Anal. Calcd for $C_{15}H_{15}N_3O_{12}Cl_2Ru$: C, 29.96; H, 2.51; N, 6.99; Cl, 11.79. Found: C, 29.87; H, 2.58; N, 6.87; Cl, 12.24.

[Ru(tpy)(H₂O)₃]²⁺. This complex was generated in situ by the Zn/Hg reduction of *trans*-[Ru(tpy)(O)₂(H₂O)](ClO₄)₂ in 0.1 M HClO₄ solution under nitrogen. We were unable to isolate it as the salt [Ru(tpy)(H₂O)₃](ClO₄)₂ from the deep red-maroon solution that resulted.

Instrumentation and Measurements. UV-visible spectra were recorded by using a Hewlett-Packard Model 8452A diode array and a CARY 14 spectrophotometer with 1-cm quartz cells. Infrared spectra were obtained by using a Nicolet Model 20DX FTIR spectrophotometer on KBr pellets or on CH₃CN solutions using NaCl plates. Resonance Raman spectra were obtained at the UNC Laser Facility. Samples were contained in NMR tubes and examined in a spinning arrangement. Raman scattering was collected at 90° to the incident radiation, which was supplied by the 454.5-nm line of a Spectra-Physics 165-05 Ar⁺ laser. Laser power was ca. 20 mW at the sample. A Jobin Yvon U1000 double monochromator (Instruments SA) was used to disperse and scan the scattered light, which was detected by a thermoelectrically cooled Hamamatsu R943-02 photomultiplier. The resulting signal was processed by an Instruments SA Spectra Link photon-counting system. Data aquisition and storage was accomplished with an IBM PS-2 Model 80 computer with an enhanced Prism Software package (Instruments SA). The symmetries of the observed resonance Raman peaks were obtained by depolarization ratio measurements. ¹H NMR spectra were obtained by using a Bruker 200AC-MHz FT-NMR spectrometer.

Electrochemical measurements were made with a Princeton Applied Research Model 173 potentiostat/galvanostat connected to a Princeton Applied Research Model 175 universal programmer as a sweep generator for voltammetric experiments. Spectroelectrochemical experiments were performed in a three-compartment electrochemical cell where the working electrode compartment was a 1-cm quartz cell. Controlled-potential electrolysis experiments were carried out by using a reticulated vitreous carbon electrode (ERG, Inc.). Cyclic voltammetric experiments were carried out in single one-compartment cells by using an "activated" Teflon-sheathed 0.07 cm² glassy-carbon-disk working electrode,[15] a platinum wire as the auxiliary electrode, and a saturated sodium chloride calomel reference electrode (SSCE). The pH of solutions was determined by using a Radiometer pHM62 pH meter and a combination pH electrode (Fisher). Buffer solutions for the electrochemical measurements were prepared from aqueous perchloric acid, HClO₄, with LiClO₄ (pH = 1–2), and HClO₄ with NaH₂PO₄·H₂O, Na₂HPO₄·7H₂O, and Na₃PO₄·12H₂O, (pH = 2–9) to maintain ionic strength at 0.1 M. The concentrations of the complexes in the cyclic voltammetric measurements were 1.0–1.5 mM. Electrochemical experiments in aqueous media for

establishing $E_{1/2}$ vs pH profiles were performed on solutions containing either [Ru(tpy)(H₂O)₃](ClO₄)₂ or *trans*-[Ru(tpy)(O)₂(H₂O)](ClO₄)₂. All cyclic voltammograms of [Ru(tpy)(H₂O)₃]²⁺ were obtained after purging with nitrogen. The $E_{1/2}$ values reported in this work were calculated from cyclic voltammetric wave forms as an average of the oxidative and reductive peak potentials, $(E_{pa} + E_{pc})/2$.

Kinetic measurements were carried out on a Hi-Tech Scientific SF-51 stopped-flow apparatus with fiber-optic coupling to either a Beckman DU or a Harrick rapid scan monochromator. The system was interfaced with a Zenith 158 microcomputer by use of On Line Instrument System (OLIS) data acquisition hardware and software. The temperature of the reactant solutions was controlled to within ±0.1 °C by using a Brinkman Lauda K-2/RD water bath circulator. Gas chromatographic analyses were carried out with a Hewlett-Packard 5890A gas chromatograph equipped with a thermal conductivity detector. Analysis for H₂O was carried out on a Porapak Q column at 150 °C with He carrier gas (35 psi).[16]

The reaction involving the equilibration of the aqua, Ru(H₂O)²⁺, and acetonitrile, Ru(NCCH₃)²⁺, complexes (eq 5) was monitored at 380, 410, and 416 nm after mixing equal volumes of 1.13×10^{-4} M of *trans*-[Ru(tpy)(O)₂(CH₃CN)]²⁺ and 1.15, 1.29, 1.44, and 1.60 M H₂O in acetonitrile solution. The kinetics of the reaction

$$Ru(H_2O)^{2+} + CH_3CN \rightleftharpoons Ru(NCCH_3)^{2+} + H_2O$$
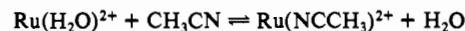
$$K = \frac{k_1}{k_{-1}} = \frac{[Ru(NCCH_3)^{2+}][H_2O]}{[Ru(H_2O)^{2+}]}$$

can be reduced to a pseudo-first-order reversible form under the conditions used experimentally with [H₂O] ≫ [Ru(NCCH₃)²⁺]. Under these conditions the approach to equilibrium was a first-order process and the first-order rate constant, k, was determined by fitting the kinetic data according to eq 1, where A_0 is the initial absorbance, A_∞ is the final

$$A_t = A_\infty + (A_0 - A_\infty)[\exp(-kt)] \tag{1}$$

absorbance after mixing, A_t is the absorbance at time t and k is the pseudo-first-order rate constant. The derived first-order rate constant is the sum of k_1 and k'_1, where $k'_1 = k_{-1}[H_2O]$. The value of k was independent of the direction from which the equilibrium was approached. The equilibrium constant, K, was determined independently from measurements of the relative integrated areas of the resonances of the 6,6″-protons of the two remote pyridyl rings of the tpy ligands. These resonances were at 9.52 ppm for the aqua complex and 9.45 for the nitrile complex vs external TMS.

Determination of the Acid Dissociation Constant. The acid dissociation constant for *trans*-[Ru(tpy)(O)₂(H₂O)]²⁺ was determined by the method described by Rosenblatt.[17] The pH was maintained with a 0.1 M phosphate buffer. This method requires absorbance measurements of solutions, at three different pH values where, $pH_{min} < pK_a < pH_{max}$. The absorbance was measured at five wavelengths, and the reported value is the average of all measurements.

Results

Syntheses. The approach taken to the synthesis of the *trans*-dioxo complex was to search for acid-sensitive precursors to [Ruᴵᴵ(tpy)(H₂O)₃]²⁺. Oxidation of the triaqua complex was expected to give the aqua-*trans*-dioxo–Ru(VI) complex

$$(tpy)Ru \overset{\displaystyle O}{\underset{\displaystyle O}{\overset{\|}{\underset{\|}{—}}}} OH_2{}^{2+}$$
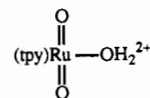
since the analogous complex of Os(VI) is known.[6c] With this thought in mind a general procedure was developed for the preparation of complexes with oxygen donor ligands based on reduction of Ru(tpy)Cl₃ by triethylammine in water/methanol mixtures in the presence of the added ligand. With the dianionic ligand C₂O₄²⁻, the neutral aqua complex was isolated.

$$Ru(tpy)Cl_3 \xrightarrow[H_2O/CH_3OH]{C_2O_4{}^{2-}/Et_3N} Ru(tpy)(C_2O_4)(H_2O)$$
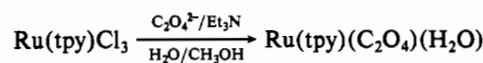
(15) (a) Diamantis, A. A.; Murphy, W. R., Jr.; Meyer, T. J. *Inorg. Chem.* **1984**, *23*, 3230. (b) Cabaniss, G. E.; Diamantis, A. A.; Murphy, W. R., Jr.; Linton, R. W.; Meyer, T. J. *J. Am. Chem. Soc.* **1985**, *107*, 1845.

(16) Hogan, J. M.; Engel, R. A.; Stevenson, H. F. *Anal. Chem.* **1970**, *42*, 249.

(17) Rosenblatt, D. H. *J. Phys. Chem.* **1954**, *58*, 40.

Table I. Ru=O Bond Distances and O=Ru=O Angles for
*trans*-[$Ru^{VI}O_2$] Complexes with N Donor Ligands

complex	Ru=O, Å	∠O=Ru=O, deg	ref
[Ru(tpy)(O)$_2$(H$_2$O)](ClO$_4$)$_2$	1.661	171	a
[Ru(py)$_2$(O$_2$CCH$_3$)$_2$(O)$_2$]	1.726	180	b
[Ru(15-TMC)(O)$_2$](ClO$_4$)$_2$	1.718	180	c
[Ru(16-TMC)(O)$_2$](ClO$_4$)$_2$	1.705	180	c

^{a} Reference 2a and this work. ^{b} Lau, T. C.; Kochi, J. K. *J. Chem. Soc., Chem. Commun.* **1987**, 798. Perrier, S.; Lau, T. C.; Kochi, J. K. *Inorg. Chem.* **1990**, *29*, 4190. ^{c} Mak, T. C. W.; Che, C.-M.; Wong, K.-Y. *J. Chem. Soc., Chem. Commun.* **1985**, 986. 15-TMC = 1,4,8,12-tetramethyl-1,4,8,12-tetraazacyclopentadecane; 16-TMC = 1,5,9,13-tetramethyl-1,5,9,13-tetraazacyclohexadecane.

For the monoanionic acetylacetonato ligand,[18] the product isolated was the monochloro complex.

$$Ru(tpy)Cl_3 \xrightarrow[CH_3OH]{acacH/Et_3N} Ru(tpy)(acac)Cl$$
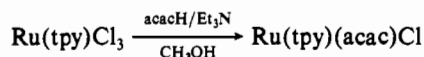
Spectrophotometric studies showed that aquation of the bound chloride occurred within minutes to give the corresponding aqua complex (eq 2).

$$Ru(tpy)(acac)Cl + H_2O \rightarrow [Ru(tpy)(acac)(H_2O)]^+ + Cl^- \quad (2)$$
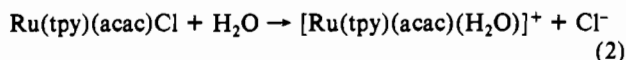
The chloro–acetylacetonato complex is stable in acidic solutions for extended periods (>1 h) toward loss of acac$^-$ and was not a useful precursor. The oxalato complex proved to be sensitive to acid hydrolysis. When it was added to acidic solutions the triaqua complex was formed quantitatively (eq 3). We were unable to

$$Ru^{II}(tpy)(C_2O_4)(H_2O) + 2H_2O + 2H^+ \rightarrow$$
$$[Ru^{II}(tpy)(H_2O)_3]^{2+} + H_2C_2O_4 \quad (3)$$
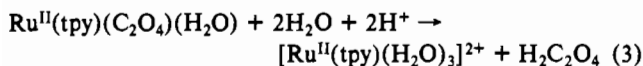
isolate the triaqua complex as a well-defined solid, but its oxidation by Ce(IV) in acidic solutions gave the desired *trans*-dioxo complex (eq 4), which was isolated as the perchlorate salt. Subsequent

$$[Ru^{II}(tpy)(H_2O)_3]^{2+} + 4Ce^{4+} \rightarrow$$
$$[Ru(tpy)^{VI}(O)_2(H_2O)]^{2+} + 4Ce^{3+} + 4H^+ \quad (4)$$
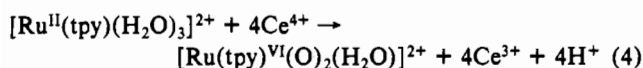
reduction of *trans*-[Ru(tpy)(O)$_2$(H$_2$O)]$^{2+}$ by Zn/Hg in acidic solution gave [Ru(tpy)(H$_2$O)$_3$]$^{2+}$ quantitatively as shown by spectrophotometric experiments.

The structure of *trans*-[Ru(tpy)(O)$_2$(H$_2$O)]$^{2+}$ has been determined by X-ray crystallography.[2a] The coordination geometry at Ru(VI) is a distorted octahedron consisting of the tpy and aqua ligands in the same plane and the two oxo ligands coordinated to Ru(VI) in a trans disposition. The average Ru=O bond length is 1.661 Å, this appears to be the shortest Ru=O bond length that has been reported (Table I). The Ru–O bond length for the terminal aqua ligand is 2.128 Å, which is in the range 2.016–2.139 Å that has been observed for the aqua ligand bound to Ru in a variety of oxidation states.[19] It is longer than the 1.957–2.036 Å lengths observed previously for terminal hydroxo groups.[20] The range of bond lengths for a terminal oxo ligand

(18) (a) Hasegawa, T.; Lau, T. C.; Taube, H.; Schaefer, W. P. *Inorg. Chem.* **1991**, *30*, 2921. For review: (b) Siedle, A. R. In *Comprehensive Coordination Chemistry*; Wilkinson, G., Gillard, R. D., McCleverty, J. A., Eds.; Pergamon: Oxford, England, 1987; Vol 2, pp 365–412. (c) Black, D. St. C. In ref 18b, Vol 6, p 202. (d) Kawaguchi, S. *Coord. Chem. Rev.* **1986**, *70*, 51.

(19) (a) Llobet, A.; Hodgson, D. J.; Meyer, T. J. *Inorg. Chem.* **1990**, *29*, 3760. (b) Seok, W. K. Ph.D. Dissertation, The University of North Carolina, Chapel Hill, NC, 1988. (c) Bernhard, P.; Burgi, H.; Hauser, J.; Lehmann, H.; Ludi, A. *Inorg. Chem.* **1982**, *21*, 3936. (d) Dong, V.; Keller, H. J.; Endress, H.; Moroni, W.; Nothe, D. *Acta Crystallogr., Sect. B* **1977**, B33, 2428.

(20) (a) Aoyagi, K.; Nagao, H.; Yukawa, Y.; Ogura, M.; Kuwayama, A.; Howell, F. S.; Mukaida, M.; Kakihana, H. *Chem. Lett.* **1986**, 2135. (b) Durham, B.; Wilson, S. R.; Hodgson, D. J.; Meyer, T. J. *J. Am. Chem. Soc.* **1980**, *102*, 600. (c) Nowogrocki, P. G.; Abraham, F.; Trehoux, J.; Thomas, D. *Acta Crystallogr., Sect. B* **1976**, B32, 2413.
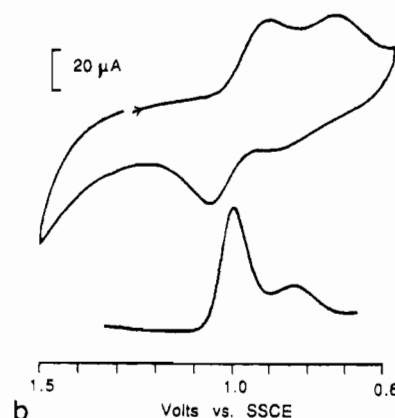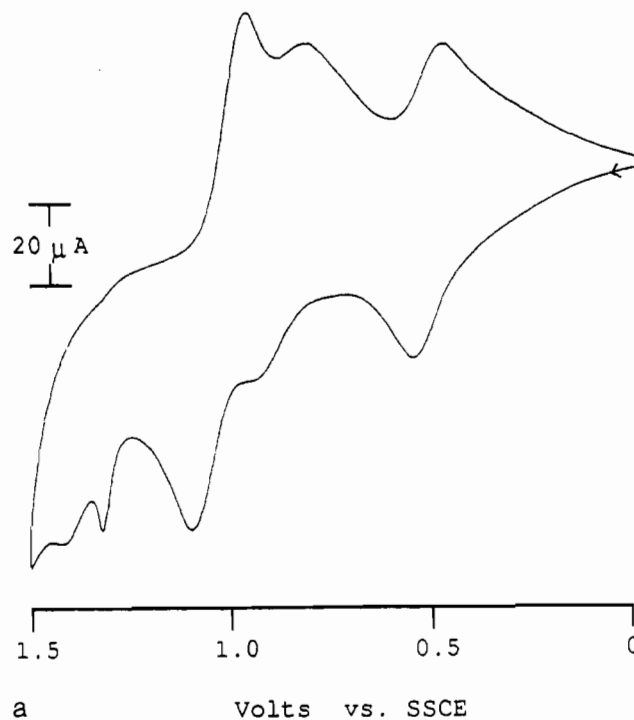
Figure 1. (a) Cyclic voltammogram of a solution 1.5 mM in [Ru^{II}(tpy)(H$_2$O)$_3$]$^{2+}$ (scan rate 100 mV s^{-1}) in 0.1 M HClO$_4$ under N$_2$. (b) Cyclic voltammogram of a solution 1.1 mM in *trans*-[Ru^{VI}(tpy)(O)$_2$(H$_2$O)]$^{2+}$ (scan rate = 100 mV s^{-1}) and differential-pulse polarogram (scan rate = 5 mV s^{-1}, pulse height = 25 mV) at pH = 1.5. Conditions: "activated" 0.07 cm^2 glassy-carbon-disk electrode, *I* = 0.1 M, potentials vs SSCE.

in Ru(IV) is 1.739–1.862 Å.[5a,b,21] The O=Ru=O angle of the *trans*-dioxo group is less than 180° (171.3°) with the bending occurring away from the tpy ligand due to the repulsive interactions of the pπ electrons of the tpy ligand with the dπ–pπ electrons of the O=Ru^{VI}=O group. The angle between the trans-N atoms in the tpy ligand and the Ru atom is considerably less than 180° (161.1°). Table I summarizes the Ru=O distances and O=Ru=O angles for complexes containing the *trans*-Ru(VI)–dioxo unit bound to N donor ligands.

Electrochemistry. At pH = 1.0 proton-catalyzed loss of the oxalato ligand is rapid and cyclic voltammograms of Ru^{II}(tpy)(C$_2$O$_4$)(H$_2$O) are those of [Ru^{II}(tpy)(H$_2$O)$_3$]$^{2+}$. The oxalato

(21) (a) Che, C. M.; Lai, T. F.; Wong, K. Y. *Inorg. Chem.* **1987**, *26*, 2289. (b) Aoyagi, K.; Yukawa, Y.; Shimizu, K.; Mukaida, M.; Takeuchi, T.; Kakihana, H. *Bull. Chem. Soc. Jpn.* **1986**, *59*, 1493. (c) Yukawa, Y.; Aoyagi, K.; Kurihara, M.; Shirai, K.; Shimizu, K.; Mukaida, M.; Takeuchi, T.; Kakihana, H. *Chem. Lett.* **1985**, 283. (d) Che, C. M.; Wong, K. Y.; Mak, T. C. W. *J. Chem. Soc., Chem. Commun.* **1985**, 546.
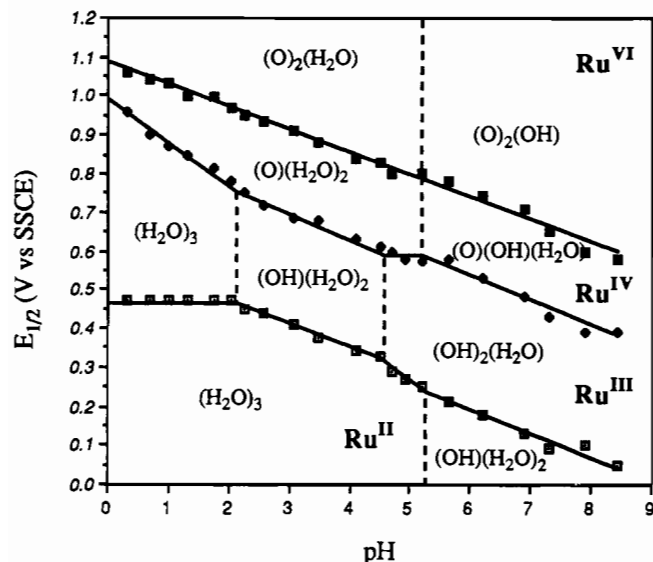
Figure 2. pH dependence of the $E_{1/2}$ values for the various couples interrelating *trans*-[Ru^{VI}(tpy)(O)$_2$(H$_2$O)]$^{2+}$ and [Ru^{II}(tpy)(H$_2$O)$_3$]$^{2+}$. The proton compositions of the various oxidation states are indicated, for example, by (H$_2$O)$_3$ for [Ru^{II}(tpy)(H$_2$O)$_3$]$^{2+}$. Vertical lines are drawn from the breaks in the $E_{1/2}$ lines and represent approximate pK_a values. The potential–pH regions where the various oxidation states are the dominant forms are indicated in the diagram.

ligand is also lost by aquation at higher pH, but on a slower time scale as shown by cyclic voltammetric and spectrophotometric measurements. The triaqua complex is air sensitive in aqueous solution. A blue, μ-oxo-bridged complex appeared in air-saturated acidic solutions within a few minutes after generating [Ru^{II}-(tpy)(H$_2$O)$_3$]$^{2+}$ by Zn/Hg reduction.[22]

A cyclic voltammogram of the triaqua complex at pH = 1.0 under N$_2$ and a scan rate of 100 mV/s shows three distinct, reversible waves (Figure 1a). The same pattern of waves has been observed for related *trans*-diaqua polypyridyl or macrocyclic ligand complexes of Ru and Os.[6a,b] From relative peak heights the waves at $E_{1/2}$ = 0.47 and 0.87 V arise from the one-electron Ru(III/II) and Ru(IV/III) couples, and the wave at $E_{1/2}$ = 1.03 V is a two-electron wave for the Ru(VI/IV) couple. The origin of the small, narrow wave at E_{pa} = 1.32 V may be from adsorption and the additional wave at E_{pa} = 1.42 V from oxidation of the adsorbate. These waves appear mainly on "activated" glassy-carbon electrode surfaces when [Ru^{II}(tpy)(H$_2$O)$_3$]$^{2+}$ is the starting complex or when it is generated in solution electrochemically.

Controlled-potential electrolysis experiments at pH = 1.0 confirmed the number of redox equivalents at each wave. Electrolysis of a solution containing [Ru^{II}(tpy)(H$_2$O)$_3$]$^{2+}$ in 0.1 M CF$_3$CO$_2$H at +0.80 V vs SSCE occurred with n = 1.0 ± 0.1, consistent with a one-electron oxidation from Ru(II) to Ru(III). Electrolysis at 1.20 V occurred with n = 3.1 ± 0.2 consistent with a three-electron oxidation from Ru(III) to Ru(VI). The UV–visible spectral changes associated with the redox processes were monitored spectroelectrochemically.

A cyclic voltammogram and a differential pulse polarogram of a solution containing *trans*-[Ru^{VI}(tpy)(O)$_2$(H$_2$O)]$^{2+}$ at pH = 1.5 are shown in Figure 1b. The wave at $E_{1/2}$ = 0.99 V arises from the Ru(VI/IV) couple and the wave at $E_{1/2}$ = 0.84 V from the Ru(IV/III) couple, which is kinetically slow at the electrode. The peak to peak potential differences between the anodic and the cathodic waves for the Ru(IV/III) couple are ΔE_p = 150 mV at a scan rate of 200 mV s^{-1}, 110 mV (100 mV s^{-1}), 90 mV (50 mV s^{-1}), and 60 mV (<20 mV s^{-1}).

In general, the potentials for the couples decrease as the pH is increased. The results of a pH dependence study are illustrated in the $E_{1/2}$–pH diagram in Figure 2, where the $E_{1/2}$ values are

(22) (a) Llobet, A.; Curry, M. E.; Evans, H. T.; Meyer, T. J. *Inorg. Chem.* **1989**, *28*, 3131. (b) Llobet, A.; Doppelt, P.; Meyer, T. J. *Inorg. Chem.* **1988**, *27*, 514. (c) Adeyemi, S. A. Unpublished results.

Table II. pK_a Values for Aqua and Hydroxo Complexes of Ru[a]

oxidn state	complex	pK_{a_1}	pK_{a_2}	ref
II	[Ru(tpy)(H$_2$O)$_3$]$^{2+}$	5.3	>8.0	d
	trans-[Ru(bpy)$_2$(H$_2$O)$_2$]$^{2+}$	9.2	>11.5	6a
	cis-[Ru(bpy)$_2$(H$_2$O)$_2$]$^{2+}$	8.9[b]	>11	6a
III	[Ru(tpy)(H$_2$O)$_3$]$^{3+}$	2.1	4.6	d
	trans-[Ru(bpy)$_2$(H$_2$O)$_2$]$^{3+}$	<1	~5.2	6a
	cis-[Ru(bpy)$_2$(H$_2$O)$_2$]$^{3+}$	~1.5	~5.2	6a
IV	[Ru(tpy)(O)(H$_2$O)$_2$]$^{2+}$	5.2	>8.0	d
	trans-[Ru(bpy)$_2$(O)(H$_2$O)]$^{2+}$	~6–7		6a
	cis-[Ru(bpy)$_2$(O)(H$_2$O)]$^{2+}$	~4–5		6a
V	*cis*-[Ru(bpy)$_2$(O)(OH)]$^{2+}$	~4.5		6a
VI	*trans*-[Ru(tpy)(O)$_2$(H$_2$O)]$^{2+}$	5.2, 5.1[c]	>8.0	d

[a] Determined from the $E_{1/2}$ – pH diagram (I = 0.1 M, 23 ± 2 °C) in Figure 2. [b] Also determined by spectrophotometric titration: Allen, L. R.; Craft, P. P.; Durham, B.; Walsh, J. *Inorg. Chem.* **1987**, *26*, 53. [c] Determined by spectrophotometric titration. [d] This work.

Table III. Summary of Reduction Potentials at Various pH Values (I = 0.1 M, 22 ± 2 °C) vs SSCE[a]

pH	redox couple	$E_{1/2}$, V
1.0	[Ru^{III}(t)(H$_2$O)$_3$]$^{3+}$/[Ru^{II}(t)(H$_2$O)$_3$]$^{2+}$	0.47
	[Ru^{IV}(t)(O)(H$_2$O)$_2$]$^{2+}$/[Ru^{III}(t)(H$_2$O)$_3$]$^{3+}$	0.87
	[Ru^{VI}(t)(O)$_2$(H$_2$O)]$^{2+}$/[Ru^{IV}(t)(O)(H$_2$O)$_2$]$^{2+}$	1.03
4.0	[Ru^{III}(t)(OH)(H$_2$O)$_2$]$^{2+}$/[Ru^{II}(t)(H$_2$O)$_3$]$^{2+}$	0.35
	[Ru^{IV}(t)(O)(H$_2$O)$_2$]$^{2+}$/[Ru^{III}(t)(OH)(H$_2$O)$_2$]$^{2+}$	0.64
	[Ru^{VI}(t)(O)$_2$(H$_2$O)]$^{2+}$/[Ru^{IV}(t)(O)(H$_2$O)$_2$]$^{2+}$	0.86
7.0	[Ru^{III}(t)(OH)$_2$(H$_2$O)]$^+$/[Ru^{II}(t)(OH)(H$_2$O)$_2$]$^+$	0.14
	[Ru^{IV}(t)(O)(OH)(H$_2$O)]$^+$/[Ru^{III}(t)(OH)$_2$(H$_2$O)]$^+$	0.47
	[Ru^{VI}(t)(O)$_2$(OH)]$^+$/[Ru^{IV}(t)(O)(OH)(H$_2$O)]$^+$	0.67

[a] t is tpy.

shown as a function of pH from pH 0 to pH 9. Above pH ∼ 9 it was difficult to obtain well-defined wave forms because of the existence of a competitive pathway, in which the formation of a μ-oxo complex or complexes occurred on the time scale of the electrochemical measurements. The lines drawn through the experimental points are of slopes of 0, −60, or −120 mV/pH unit. These slopes are predicted by the Nernst equation in the form, $E^{\circ\prime} = E_{1/2} - 0.05916(m)/(n)(\text{pH})$, where m is the number of protons, n is the number of electrons, and $E_{1/2}$ is the half-wave potential at pH = 0.[23] In the diagram the pH contents, regions of stability for the various oxidation states, and proton compositions are indicated. For example, the label (H$_2$O)$_3$ in the Ru^{II} region represents the cation [Ru^{II}(tpy)(H$_2$O)$_3$]$^{2+}$. The vertical dashed lines indicate the pK_a's of the corresponding complex, for example, the pK_a for the first proton loss from [Ru^{II}(tpy)(H$_2$O)$_3$]$^{2+}$ is 5.3.

$$[\text{Ru}^{II}(\text{tpy})(\text{H}_2\text{O})_3]^{2+} \rightleftharpoons [\text{Ru}^{II}(\text{tpy})(\text{OH})(\text{H}_2\text{O})_2]^+ + \text{H}^+$$

In Table II are listed the pK_a values that were estimated from the break points in the $E_{1/2}$ vs pH profiles. Values for related complexes based on *cis*-[Ru^{VI}(bpy)$_2$(O)$_2$]$^{2+}$ and *trans*-[Ru^{VI}-(bpy)$_2$(O)$_2$]$^{2+}$ are also included for comparison. The acid dissociation constant for *trans*-[Ru^{VI}(tpy)(O)$_2$(H$_2$O)]$^{2+}$ was determined by spectrophotometry to be pK_a = 5.1 ± 0.1 which is in good agreement with the value 5.2 determined from the break in the $E_{1/2}$ vs pH plot for the Ru(VI/IV) couple. Reduction potentials for all the redox couples at various pH values are listed in Table III. They were determined by measurements in solutions containing either [Ru^{II}(tpy)(H$_2$O)$_3$]$^{2+}$ or *trans*-[Ru^{VI}(tpy)(O)$_2$-(H$_2$O)]$^{2+}$.

Electronic Absorption Spectra. The absorption spectrum of *trans*-[Ru^{VI}(tpy)(O)$_2$(H$_2$O)]$^{2+}$ (Figure 3a) in aqueous solution includes a transition at λ_{max} = 410 nm, ϵ = 3700 M^{-1} cm^{-1}, in H$_2$O (pH = 1.0). In CH$_3$CN, where the aqua group is replaced by CH$_3$CN, the band shifts to λ_{max} = 416 nm, ϵ = 3500 M^{-1} cm^{-1}. The intense bands in the UV region (Table IV) have been assigned to ligand (tpy) based $\pi \rightarrow \pi^*$ transitions.[24] The absorption
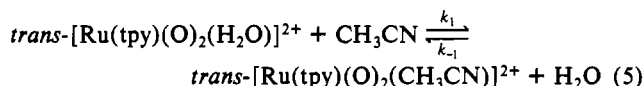
(23) Bard, A. J.; Faulkner, L. R. *Electrochemical Methods*; John Wiley: New York, 1980; p 213.
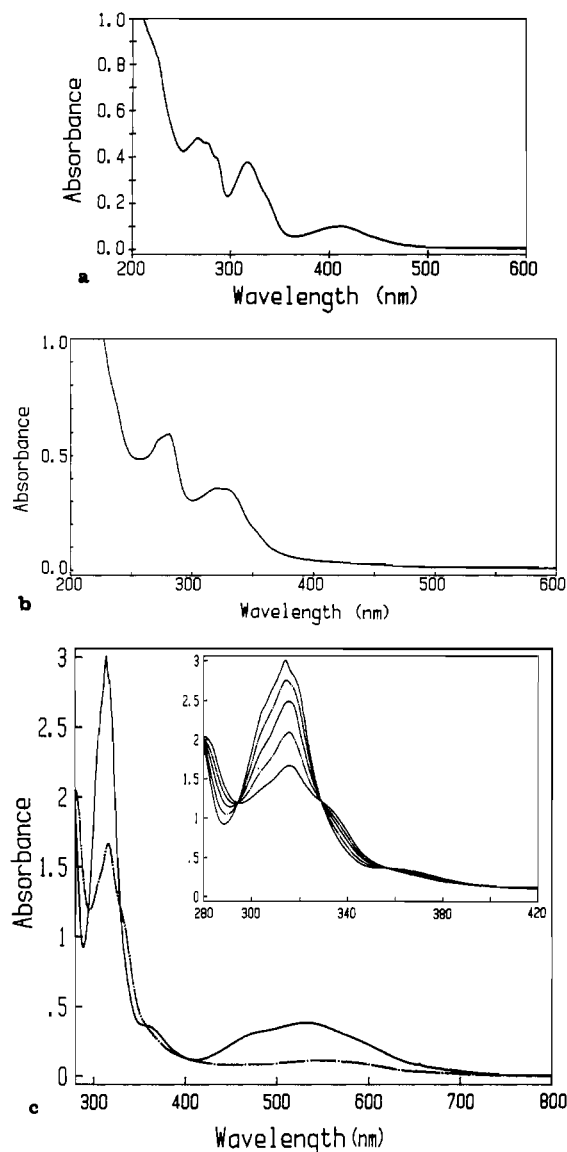
Figure 3. Electronic absorption spectra of (a) *trans*-[Ru^VI(tpy)(O)₂-(H₂O)]²⁺, at pH = 1.0, (b) [Ru^IV(tpy)(O)(H₂O)₂]²⁺, at pH = 1.0, and (c) [Ru^II(tpy)(H₂O)₃]²⁺ (—) and [Ru^III(tpy)(H₂O)₃]³⁺ (—·—) at pH = 1.0. Inset: spectrophotometric titration of [Ru^II(tpy)(H₂O)₃]²⁺ by Ce-(IV) (0.00 (top spectrum), 0.20, 0.40, 0.70, and 1.00 equiv of Ce(IV)) in 0.1 M HClO₄–0.05 M NaClO₄. Extinction coefficient values are given in Table IV.

spectrum of [Ru^IV(tpy)(O)(H₂O)₂]²⁺ at pH = 1.0 is shown in Figure 3b. The spectra of [Ru^II(tpy)(H₂O)₃]²⁺ and [Ru^III-(tpy)(H₂O)₃]³⁺ and the results of a spectrophotometric titration of Ru(II) by 1 equiv of Ce(IV) at pH = 1.0 are also shown in Figure 3c. In Table IV are listed in a summary fashion the UV–visible spectral properties of the various complexes.

Equilibrium and Rate Constants for the Equilibrium between H₂O and CH₃CN. The kinetics of the reaction between *trans*-[Ru^VI(tpy)(O)₂(CH₃CN)]²⁺ and H₂O in acetonitrile were found to be first order with respect to both reactants.

$$\textit{trans-}[\text{Ru(tpy)(O)}_2(\text{H}_2\text{O})]^{2+} + \text{CH}_3\text{CN} \underset{k_{-1}}{\overset{k_1}{\rightleftharpoons}}$$

$$\textit{trans-}[\text{Ru(tpy)(O)}_2(\text{CH}_3\text{CN})]^{2+} + \text{H}_2\text{O} \quad (5)$$

The observed rate constant, $k = k_1 + k_{-1}[\text{H}_2\text{O}]$, varied linearly with water concentration with slope $k_{-1} = 35.3 \pm 0.1$ M⁻¹ s⁻¹ (19.5

(24) (a) Suen, H. F.; Wilson, S. W.; Pomerantz, M.; Walsh, J. L. *Inorg. Chem.* **1989**, *28*, 786. (b) Takeuchi, K. J.; Thompson, M. S.; Pipes, D. W.; Meyer, T. J. *Inorg. Chem.* **1984**, *23*, 1845. (c) Thompson, M. S. Ph.D. Dissertation, The University of North Carolina, Chapel Hill, NC, 1981.

Table IV. Visible and Ultraviolet Spectrophotometric Parameters in CH₃OH or 0.1 M HClO₄

complex	λ_{max}, nm (ϵ_{max}, M⁻¹ cm⁻¹)
	In CH₃OH
[Ru(tpy)(acac)Cl]	610 (sh, 546 (3850), 386 (5350), 318 (17 100), 278 (20 800), 232 (22 500), 210 (26 500)
[Ru(tpy)(C₂O₄)(H₂O)]	580 (3800), 528 (4200), 380 (5600), 320 (25 800), 310 sh, 275 (19 900)
	0.1 M HClO₄ in H₂O
[Ru(tpy)(acac)(H₂O)]⁺	542 (3000), 370 sh, 317 (20 050), 272 (25 000), 233 (20 000)
[Ru(tpy)(H₂O)₃]²⁺	532 (3450), 470 sh, 360 sh, 314 (30 500), 274 (20 000), 232 (19 000)
[Ru(tpy)(H₂O)₃]³⁺	544 (950), 314 (18 000), 274 (20 000), 232 sh, 216 (45 000)
[Ru(tpy)(O)(H₂O)₂]²⁺	330 (10 900), 320 (11 200), 280 (18 000)
trans-[Ru(tpy)(O)₂(H₂O)]²⁺	410 (3700), 340 sh, 316 (13 400), 285 sh, 275 sh, 265 (16 900), 225 sh

Table V. Rate and Equilibrium Constants for the Equilibration between *trans*-[Ru(tpy)(O)₂(CH₃CN)]²⁺ and *trans*-[Ru(tpy)(O)₂(H₂O)]²⁺ in Acetonitrile Solutions at 19.5 °C

[complex], mM	[H₂O], M^a	k, s⁻¹ ᵇ	N^c	K, M^d
0.113	1.15	45.5 ± 0.2	10	
	1.29	50.4 ± 0.2	9	
	1.44	55.8 ± 0.1	8	0.15 ± 0.01
	1.60	61.4 ± 0.1	9	

ᵃ [H₂O] was measured by GC. ᵇ The reaction was monitored at λ = 416, 410, and 380 nm. The observed rate constant was independent of wavelength. ᶜ N is the number of replicates averaged. ᵈ K was determined from ¹H NMR studies in CD₃CN solution at various [H₂O] (see Experimental Section).
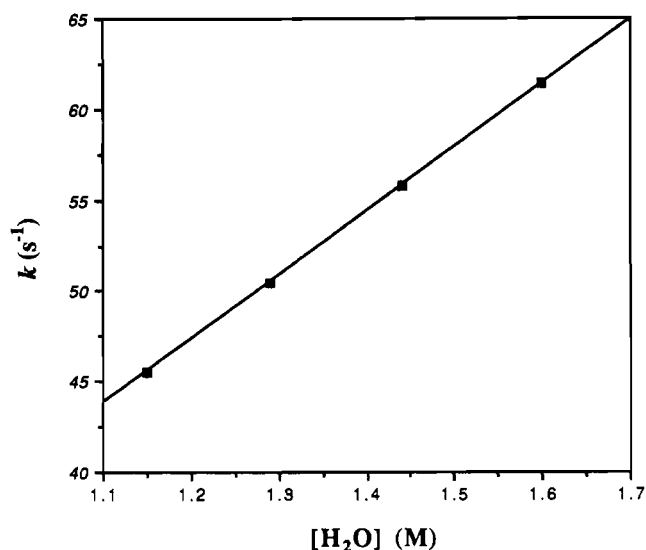
Figure 4. Variation of the observed rate constant at 19.5 °C for the equilibration between *trans*-[Ru^VI(tpy)(O)₂(CH₃CN)]²⁺ and *trans*-[Ru^VI(tpy)(O)₂(H₂O)]²⁺ in acetonitrile as a function of the concentration of added water.

°C) and intercept $k_1 = 4.9 \pm 0.2$ s⁻¹ (Figure 4). The ratio of rate constants is in good agreement with the equilibrium constant, $K = 0.15 \pm 0.01$ M, which was determined independently by ¹H NMR studies in D₂O/CD₃CN mixtures. In Table V are summarized the results of the rate and equilibrium constant studies on the equilibrium in eq 5.

¹H NMR, Resonance Raman, and Infrared Spectra. The ¹H NMR spectrum in the terpyridine region for *trans*-[Ru^VI(tpy)-(OH)(O)₂]⁺ in D₂O (pD = 7.5) is consistent with a diamagnetic complex with tpy resonances appearing at 9.17 ppm (dd, J_{56} = 5.6 Hz, J_{46} = 1.3 Hz, 2 H, H₆, H₆′′), at 8.70 ppm (multiplet, 5 H, H₃, H₃′′, H₄′, H₅′, H₃′), at 8.51 ppm (ddd, J_{45} = 7.9 Hz, J_{43} = 8 Hz, J_{46} = 1.3 Hz, 2 H, H₄, H₄′′), and at 8.02 ppm (ddd, J_{56}

Table VI. Asymmetric and Symmetric Stretches of *trans*-[Ru^{VI}O$_2$] Complexes with N Donor Ligands

complex	ν_{sym}(RuO$_2$), cm^{-1}	ν_{asym}(RuO$_2$), cm^{-1}	ref
[Ru(tpy)(O)$_2$(H$_2$O)](ClO$_4$)$_2$	834	841	a
[Ru(tpy)(O)$_2$(CH$_3$CN)](ClO$_4$)$_2$	825	837	a
[Ru(py)$_4$(O)$_2$](BF$_4$)$_2$	818	840	b
[Ru(py)$_2$(Cl)$_2$(O)$_2$]	836	837	b
[Ru(py)$_2$(Br)$_2$(O)$_2$]	835	840	b
[Ru(py)(Cl)$_3$(O)$_2$](Hpy)	833	837	c
[Ru(TMP)(O)$_2$]		821	d
[Ru(L)(O)$_2$](ClO$_4$)$_2$		865	e
[Ru(L')(O)$_2$](ClO$_4$)$_2$		850	f
[Ru(py)$_2$(O$_2$CCH$_3$)$_2$(O)$_2$]		841	g
[Ru(bpy)$_2$(O)$_2$](ClO$_4$)$_2$		850	h
[Ru(py)$_4$(O)$_2$(OH)$_2$]	790	850	i

^{a} This work. ^{b} Reference 8b. ^{c} Reference 8c. ^{d} Reference 4c. ^{e} Reference 5a. L = 1,12-dimethyl-3,4:9,10-dibenzo-1,12-diaza-5,8-dioxacyclopentadecane. ^{f} Reference 5c, L' = *N,N,N',N'*-tetramethyl-3,6-dimethyl-3,6-diazaoctane-1,8-diamine. ^{g} Reference 8d. ^{h} Che, C, M.; et al. *Inorg. Chem.* **1986**, *25*, 345. ^{i} Griffith, W. P.; Rossetti, R. *J. Chem. Soc., Dalton Trans.* **1972**, 1449.

= 5.7 Hz, J_{45} = 7.9 Hz, J_{53} = 1.4 Hz, 2 H, H$_5$, H$_{5''}$). The terpyridine resonances were assigned by analysis of peak multiplicity and coupling constants.[25] The doublet that appears at low fields and integrates for two protons can be assigned to the 6,6''-protons of the two remote pyridyl groups of the terpyridyl ligand. The same pattern has been observed for related polypyridyl complexes of Ru(VI) and Os(VI).[6] The absence of paramagnetically shifted peaks in the ^{1}H NMR is expected for C_{2v} symmetry in the d^2 electronic configuration with the d$_{xy}$ orbital lower in energy relative to d$_{xz}$, d$_{yz}$ and the *trans*-dioxo bonding axis defined as the z axis.
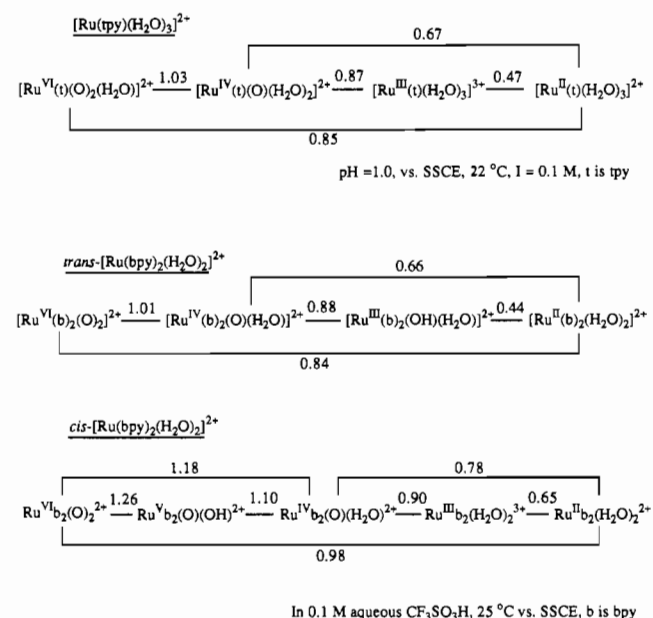
In the resonance Raman spectrum of *trans*-[Ru^{VI}(tpy)(O)$_2$-(H$_2$O)](ClO$_4$)$_2$ in the solid state the symmetric mode for the *trans*-dioxo group appears at 834 cm^{-1}. In the infrared spectrum of the salt in a KBr pellet the asymmetric mode appears at 841 cm^{-1}. In CH$_3$CN where *trans*-[Ru^{VI}(tpy)(O)$_2$(CH$_3$CN)]$^{2+}$ is formed, the symmetric mode appears at 825 cm^{-1} and the asymmetric mode at 837 cm^{-1}. From depolarization ratios the Raman-active mode is a symmetrical stretch as expected for a molecule of the type *trans*-[MO$_2$L$_4$].[26] The asymmetric and symmetric stretches of related *trans*-dioxo complexes of Ru(VI) are listed in Table VI for comparison.

Discussion

The strategy adopted for the preparation of trans-[Ru^{VI}-(tpy)(O)$_2$(H$_2$O)]$^{2+}$ was successful. The complex is an addition to a growing family of higher oxidation state oxo complexes of ruthenium and osmium. This family includes the bis(bipyridyl) complexes cis- and *trans*-[M(bpy)$_2$(O)$_2$]$^{2+}$ (M = Ru, Os),[6,27] the porphyrin complex Ru(TPP)(O)$_2$ (TPP is tetraphenylporphyrin),[4] and a series of macrocyclic complexes.[5]

From the $E_{1/2}$ vs pH plot in Figure 2, oxidation states VI → II are accessible in the pH domain 0–5 over a potential range of ~0.55 V. The key to the accessibility of the higher oxidation states is electronic donation from the hydroxo and oxo groups that are formed when protons are lost. The reduction potentials that interrelate the various couples at pH = 1 are shown in the Latimer

(25) (a) Constable, E. C. *J. Chem. Soc., Dalton Trans.* **1985**, 2687. (b) Lytle, F. E.; Petrosky, L. M.; Carlson, L. R. *Anal. Chim. Acta* **1971**, *57*, 239.

(26) (a) Brewer, J. C.; Thorp, H. H.; Slagle, K. M.; Brudvig, G. W.; Gray, H. B. *J. Am. Chem. Soc.* **1991**, *113*, 3171. (b) Thorp, H. H.; Van Houten, J.; Gray, H. B. *Inorg. Chem.* **1989**, *28*, 889. (c) Winkler, J. R.; Gray, H. B. *Inorg. Chem.* **1985**, *24*, 346.

(27) Theoretical analysis of the oxidation of olefins by cis- and trans-Ru(VI)–dioxo complexes: Cundari, T. R.; Drago, R. S. *Inorg. Chem.* **1990**, *29*, 2303.

(28) (a) Binstead, R. A.; Meyer, T. J. *J. Am. Chem. Soc.* **1987**, *109*, 3287. (b) Moyer, B. A.; Meyer, T. J. *Inorg. Chem.* **1981**, *20*, 436. (c) Bernhard, P.; Lehmann, H.; Ludi, A. *J. Chem. Soc., Chem. Commun.* **1981**, 1216. (d) Lin, C. T.; Böttcher, W.; Chou, M.; Creutz, C.; Sutin, N. *J. Am. Chem. Soc.* **1976**, *98*, 6536.

Scheme I

pH =1.0, vs. SSCE, 22 °C, I = 0.1 M, t is tpy

In 0.1 M aqueous CF$_3$SO$_3$H, 25 °C vs. SSCE, b is bpy

diagram in Scheme I and are compared with related couples based on *cis*-[Ru^{VI}(bpy)$_2$(O)$_2$]$^{2+}$ and *trans*-[Ru^{VI}(bpy)$_2$(O)$_2$]$^{2+}$.
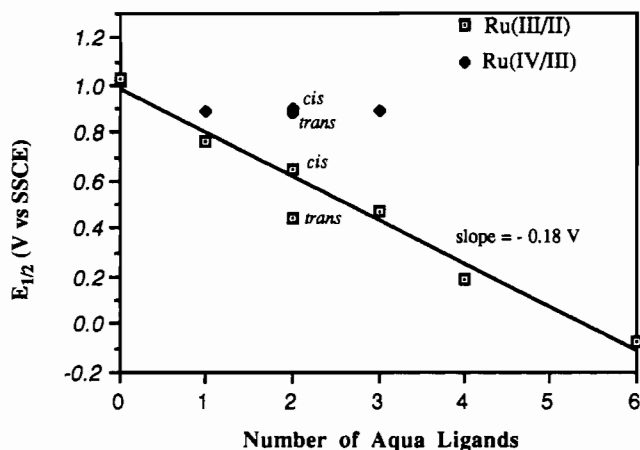
From the data in Scheme I, redox potentials for all the couples of trans-[Ru^{VI}(tpy)(O)$_2$(H$_2$O)]$^{2+}$ in acidic solutions are within or nearly within experimental error of the potentials for analogous couples based on *trans*-[Ru^{II}(bpy)$_2$(H$_2$O)$_2$]$^{2+}$. From this observation it can be inferred that exchange of the aqua group trans to tpy by the fourth pyridyl group in *trans*-[Ru^{II}(bpy)$_2$(H$_2$O)$_2$]$^{2+}$ has a negligible effect on redox potentials. This observation can be rationalized based on the orbitals involved. In Ru(II), dπ → π^* back-bonding effects are important. If the z axis is taken to lie along the H$_2$O–Ru–OH$_2$ bond axis, the order of increasing energy is predicted to be d$_{xz}$, d$_{yz}$ < d$_{xy}$ because of the inability of d$_{xy}$ to back-bond significantly to bpy. Since oxidation of dπ^6 Ru(II) occurs at d$_{xy}$ and it is unable to discriminate between H$_2$O and pyridine in a significant way, the Ru(III/II) couple is relatively unaffected by the exchange. In the higher oxidation states containing hydroxo or oxo ligands, electron donation from these ligands and dπ(Ru)–pπ(O) mixing impart antibonding character to d$_{xz}$, d$_{yz}$ which leads to the ordering d$_{xz}$, d$_{yz}$ > d$_{xy}$. Since neither H$_2$O nor pyridine is a good π donor and both are comparable as σ donors, the exchange of one for the other provides a minimal discrimination in the higher oxidation state couples. The same observations have been made in comparing potentials for the complexes *trans*-[Os^{VI}(bpy)$_2$(O)$_2$]$^{2+}$ [6b] and *trans*-[Os^{VI}(tpy)(O)$_2$(H$_2$O)]$^{2+}$. [6c]

The situation is different for *cis*-[Ru^{VI}(bpy)$_2$(O)$_2$]$^{2+}$. As shown by the data in Scheme I there are significant increases in the potentials for its Ru(III/II) and Ru(VI/IV) couples compared with those for *trans*-[Ru^{VI}(tpy)(O)$_2$(H$_2$O)]$^{2+}$. For the Ru(III/II) couple the expected orbital ordering is d$_{xz}$, d$_{yz}$ < d$_{xy}$ but d$_{xy}$ participates in dπ–π^* back-bonding with bpy in Ru(II). The exchange of H$_2$O for a back-bonding ligand in this geometry decreases the energy of d$_{xy}$, which contributes to the increase in the Ru(III/II) potential.

The influence of the exchange of a pyridyl ligand by an aqua ligand is illustrated by the correlation in Figure 5 for a series of Ru(III/II) and Ru(IV/III) couples. One feature is the decrease in oxidizing strength for the *trans*-Ru(III/II) couple compared to *cis*-Ru(III/II), of 0.21 V because of the loss of back-bonding at Ru(II) in the trans configuration.[29] For the analogous complexes of Os the difference is 0.19 V.[6c] Another feature is the

(29) (a) Taube, H. *Pure Appl. Chem.* **1979**, *51*, 901. (b) Taube, H. *Surv. Prog. Chem.* **1973**, *6*, 1. (c) Buckingham, D. A.; Sargeson, A. M. In *Chelating Agents and Metal Chelates*; Dwyer, F. P., Mellor, D. R., Eds.; Academic: New York, 1964; Chapter 6.

Figure 5. Plot of $E_{1/2}$ values[6a,28] (pH = 1.0, vs SSCE) for the Ru-(III)/Ru(II) couples $[Ru(bpy)_3]^{3+/2+}$ (in 1 M H_2SO_4), cis-$[Ru(bpy)_2$-$(py)(H_2O)]^{3+/2+}$, cis- and trans-$[Ru(bpy)_2(H_2O)_2]^{3+/2+}$, $[Ru-(tpy)(H_2O)_3]^{3+/2+}$, trans-$[Ru(py)_2(H_2O)_4]^{3+/2+}$, and $[Ru(H_2O)_6]^{3+/2+}$ and for the Ru(IV)/Ru(III) couples cis-$[Ru(bpy)_2(py)(O)]^{2+}$/cis-$[Ru-(bpy)_2(py)(H_2O)]^{3+}$, cis- and trans-$[Ru(bpy)_2(O)(H_2O)]^{2+}$/cis- and trans-$[Ru(bpy)_2(H_2O)_2]^{3+}$, and $[Ru(tpy)(O)(H_2O)_2]^{2+}$/$[Ru-(tpy)(H_2O)_3]^{3+}$.

decrease in $E_{1/2}$ for the Ru(III/II) couples of 0.18 V as a pyridyl group is replaced by an aqua group. A major contributor to this decrease is the loss of stabilization by backbonding at Ru(II) as pyridyl ligands are lost. A related trend exists for the analogous Os(III/II) couples, but the decrease in $E_{1/2}$ is 0.22 V as a pyridyl group is replaced by an aqua group.[6c] This is probably a reflection of stronger $d\pi(M) \rightarrow \pi^*$ back-bonding for Os(II).

A striking feature in the data in Figure 5 is the invariance in the Ru(IV/III) couples to the exchange of pyridyl groups for aqua or to a change in geometry from cis to trans. This is a consequence of an absence of significant metal to ligand back-bonding effects and of the similarity between pyridine and H_2O as σ donors. From this result is can be inferred that there is essentially no preference of H_2O vs pyridine for the Ru(IV/III) couples *nor for the relative disposition of pyridine vs H_2O, whether cis or trans, relative to the oxo group.* The situation is different for Os where Os(IV) is destabilized relative to Ru(IV) and potentials for the Os(IV/III) couples decrease by 0.18 V as H_2O is exchanged by pyridine.[6c]

For the Ru(VI/IV) couples it is reasonable to assume that there should be a continued lack of discrimination between pyridyl and aqua ligands on reduction potentials. If this is the case, it can be inferred from the data in Scheme I that $E_{1/2}$ for the couple cis-$[Ru^{VI}(tpy)(O)_2(H_2O)]^{2+}$/cis-,trans-$[Ru^{IV}(tpy)(O)(H_2O)_2]^{2+}$ is favored over $E_{1/2}$ for trans-$[Ru^{VI}(tpy)(O)_2(H_2O)]^{2+}$/cis-$[Ru^{IV}(tpy)(O)(H_2O)_2]^{2+}$ by ~0.17 eV.

Over the pH range that could be studied, Ru(V) is unstable with respect to disproportionation into Ru(VI) and Ru(IV) and must be a stronger oxidant than Ru(VI).[6]
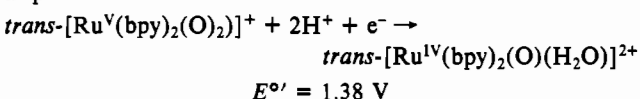
$$2Ru(V) \rightarrow Ru(VI) + Ru(IV)$$
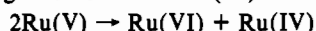
This is also true for the analogous osmium complex.[6c] From the known potential for the couple

trans-$[Ru^{VI}(bpy)_2(O)_2]^{2+} + 2H^+ + 2e^- \rightarrow$
$$trans\text{-}[Ru^{IV}(bpy)_2(O)(H_2O)]^{2+}$$
$$E_{1/2} = 1.01 \text{ V}$$
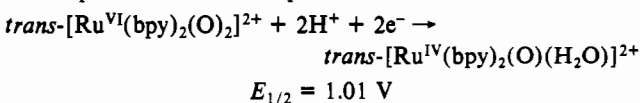
at pH = 1,[6a] the measured potential for the pH-independent (VI/V) couple

trans-$[Ru^{VI}(bpy)_2(O)_2]^{2+} + e^- \rightarrow trans\text{-}[Ru^V(bpy)_2(O)_2]^+$
$$E_{1/2} = 0.71 \text{ V}$$
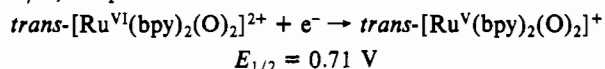
and the calculated potential for the (V/IV) couple listed below, at pH = 1

trans-$[Ru^V(bpy)_2(O)_2)]^+ + 2H^+ + e^- \rightarrow$
$$trans\text{-}[Ru^{IV}(bpy)_2(O)(H_2O)]^{2+}$$
$$E^{\circ\prime} = 1.38 \text{ V}$$

it is possible to calculate the disproportionation equilibrium constant ($\Delta G^{\circ\prime} = 0.60$ eV) $K_{dispr}(22 °C, pH = 1) = 1.5 \times 10^{10}$ for the equilibrium in eq 6. A comparable value can be expected

2 trans-$[Ru^V(bpy)_2(O)_2]^+ + 2H^+ \rightleftharpoons$
$$trans\text{-}[Ru^{VI}(bpy)_2(O)_2]^{2+} + trans\text{-}[Ru^{IV}(bpy)_2(O)(H_2O)]^{2+}$$
$$\tag{6}$$
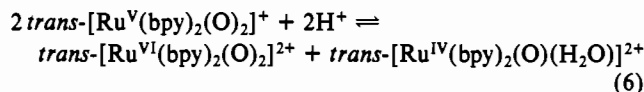
for disproportionation of trans-$[Ru^V(tpy)(O)_2(H_2O)]^+$ if the exchange of H_2O for pyridyl shifts the potentials of the Ru(VI/V) and Ru(V/IV) couples negligibly. A significant factor destabilizing Ru(V) is its electronic configuration $(d_{xy})^2 (d_{xz}, d_{yz})^1$ in which an electron resides in a strongly antibonding $d\pi$ orbital.

There is a similarity in the pattern of stable oxidation states with the structurally equivalent osmium complex, trans-$[Os^{VI}-(tpy)(O)_2(H_2O)]^{2+}$. There are also differences that can be attributed to differences in electronic and bonding properties between the two metals[30] and to the relative instability of Os(IV).[6c] Because of a difference in pH dependences for the Os(VI/V) and Os-(V/III) couples, an Os(VI/V) couple and Os(V) as a stable oxidation state appear above pH = 11. Similar behavior is expected for trans-$[Ru^{VI}(tpy)(O)_2(H_2O)]^{2+}$, but we were unable to extend the cyclic voltammetric measurements to sufficiently high pH's to see this effect. Also, in contrast to trans-$[Os^{VI}(tpy)-(O)_2(H_2O)]^{2+}$, which protonates at pH < 2.4, there is no sign of protonation of trans-$[Ru^{VI}(tpy)(O)_2(H_2O)]^{2+}$ up to pH = 0.

Implications for Reactivity. A number of features that appear in the thermodynamic analysis relate directly to reactivity. If the data in Scheme I for the cis- and trans-$[Ru^{VI}(bpy)_2(O)_2]^{2+}$-based couples are relevant to those for cis- and trans-$[Ru^{VI}(tpy)(O)_2-(H_2O)]^{2+}$, $K = 10^{-7}$, for the trans $\rightleftharpoons$ cis equilibrium in eq 7. This

trans-$[Ru(tpy)(O)_2(H_2O)]^{2+} \rightleftharpoons cis\text{-}[Ru(tpy)(O)_2(H_2O)]^{2+}$
$$\tag{7}$$
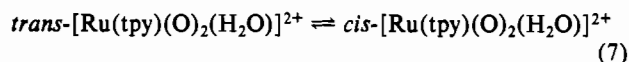
$$\Delta G^\circ \sim -0.34 \text{ eV}$$

value can be calculated from the potentials for the cis-Ru(VI/IV) and trans-Ru(VI/IV) couples by assuming that cis-Ru(IV) and trans-Ru(IV) have the same free energy content.

From the magnitude of K the cis isomer may be a more powerful two-electron oxidant than trans (by ~0.17 V), but it is present in only small amounts at equilibrium in solution and may not play a significant role in many oxidations. A mechanism that involves initial trans $\rightarrow$ cis interconversion followed by a rate-limiting redox step would necessarily have an added increment of 0.34 eV (9 kcal mol^{-1}) in its overall free energy of activation compared to a direct reaction with the trans isomer. In the limit of a substrate that is reactive and possesses a high selectivity toward oxidation by the cis isomer compared to the trans isomer, the cis $\rightarrow$ trans interconversion could become rate limiting.

The fact that Ru(V) is unstable with respect to disproportionation shows that Ru(V), presumably as $[Ru^V(tpy)(O)_2(H_2O)]^+$ in acidic solution, is a stronger oxidant than trans-$[Ru^{VI}(tpy)-(O)_2(H_2O)]^{2+}$. In mechanisms that involve initial one-electron transfer, the Ru(VI) $\rightarrow$ Ru(V) step involves a *weaker* oxidant than the second, Ru(V) $\rightarrow$ Ru(IV). This fact may tend to favor two-electron pathways and the direct formation of Ru(IV) from Ru(VI) without the intervention of Ru(V).

From the electrochemical data the preference for the trans-oxo stereochemistry in oxidation state VI of ~0.34 eV is lost at Ru(IV).
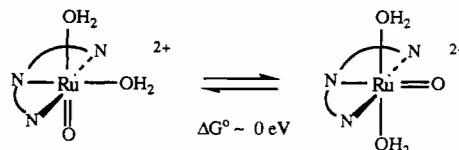
From the electrochemical comparisons the free energy difference between the two isomers formed by reduction of cis-Ru(VI) and trans-Ru(VI) must be small. This may be an important point

(30) Sullivan, B. P.; Meyer, T. J. *Inorg. Chem.* **1982**, *21*, 1037.

mechanistically. It returns to the original point of this paper and to the design of *trans*-[Ru^{VI}(tpy)(O)$_2$(H$_2$O)]$^{2+}$ as a potential cis-directed four-electron oxidant. In order for this reactivity to appear, the transfer of the remaining oxo group at Ru(IV) must occur to the plane of the tpy ligand following reduction of Ru(VI) to Ru(IV). This could occur, for example, by intramolecular proton transfer. These issues are currently under investigation.

Contribution from the Departments of Chemistry, University of Leicester, Leicester LE1 7RH, U.K., and University of New Hampshire, Durham, New Hampshire 03824-3598

The Iron(II)–Diimine Complex [Fe(CH₃N=CHCH=NCH₃)₃]²⁺: Its Structure and Its Solvation and Reactivity in Aqueous–Organic Solvent Mixtures

Michael J. Blandamer,[†] John Burgess,[†] John Fawcett,[†] Pilar Guardado,[†,‡] Colin D. Hubbard,*,[§] Sumchairuk Nuttall,[†] Lesley J. S. Prouse,[†] Stojan Radulović,[†] and David R. Russell[†]

Tris (*N,N'*-dimethylglyoxal diimine)iron(II) (Fe(gmi)₃²⁺) salts have been prepared, and the structure of the tetrafluoroborate salt has been determined by an X-ray diffraction study. Fe(gmi)₃(BF₄)₂, C₁₂H₂₄N₆B₂F₈Fe, is rhombohedral and crystallizes in space group *R3̄c*, and there are six molecules per cell. In addition the structure of [Fe(bmi)₃](ClO₄)₂ (C₁₈H₃₆N₆O₈Cl₂Fe, trigonal, space group *P3̄c1*, two molecules per cell), where the bmi ligand (*N,N'*-dimethyl-2,3-butanedione diimine) is the dimethyl analogue of gmi, has been determined so that together with available structural data for other iron(II)–diimine complexes the general reactivity of the Fe(gmi)₃²⁺ cation on the basis of structural information may be ascertained. Dissociation of Fe(gmi)₃²⁺ in the presence of hydroxide ion has been studied spectrophotometrically. The second-order rate constant, k_2 (the reaction is first order in both reactants under the conditions studied), was determined for several aqueous mono-ol mixtures and in aqueous acetone. The trend of a sharp increase in k_2 with increasing organic cosolvent content was observed; destabilization of hydroxide is a significant contributing factor. Solubility measurements were made using the perchlorate salt of the complex ion. These results, in conjunction with the TATB extrathermodynamic assumption, afforded the transfer chemical potentials for the initial state, and in combination with appropriate kinetic data those for the transition state. The reactivity trends are controlled more or less equivalently by an increasing destabilization of the overall initial state and a stabilized transition state with increasing cosolvent for aqueous ethanol, 2-propanol, and *tert*-butyl alcohol mixtures. Kinetic measurements at pressures up to 1 kbar yielded ΔV^* of +16 cm³ mol⁻¹ for dissociation by hydroxide ion in aqueous solution. ΔV^* is lowered by all cosolvents added, the value declining to +4 cm³ mol⁻¹ at the highest practicable cosolvent concentration.

Introduction

Medium effects on reactivity have been studied for a large number of reactions, organic and inorganic. Explanations of these effects have been offered in terms of a great variety of solvent properties and parameters. Most treatments deal with rate constant and activation parameter trends, but several authors have recognized that such kinetic parameters are composite quantities, representing differences between effects on initial and transition states.[1,2] Analysis of solvent effects on reactivities in these terms should lead to fuller understanding. In parallel with this approach, it is becoming increasingly recognized that solvation may have a marked effect on the pressure dependence of reactivities.[3] For a reaction of established mechanism, solvation effects can be probed through variation of activation volume with solvent nature or composition. These two approaches are complementary, in that the initial-state–transition-state analysis gives information on solvation changes for the initial state and transition state separately, on transfer from one medium to another, whereas the activation volume can give an idea of solvation changes on going from the initial state to the transition state in a given medium. This is illustrated in Figure 1, which also recalls that thermodynamic measurements, such as solubilities, are required to obtain information on transfer of the initial state, and solvent effects on the transition state can be derived from these measurements and the observed rate constants.[2] In the present paper we illustrate these approaches through the study of solvent effects on base hydrolysis of a low-spin iron(II)–diimine complex in several series of binary aqueous solvent mixtures.

The kinetics of substitution at the low-spin iron(II)–diimine complexes Fe(phen)₃²⁺ (phen = **1**) and Fe(bpy)₃²⁺ (bpy = **2**) have been extensively studied since the early days of inorganic kinetics.[4] The first studies were in aqueous solution, but subsequently solvolysis, base hydrolysis, and nucleophilic attack by cyanide have been studied in many nonaqueous and mixed aqueous media.[5] The range of diimine ligands can readily be extended by the use of Schiff bases (sb) derived from pyridine-2-aldehyde and 2-keto derivatives, **3** with R = H, CH₃, C₆H₅ and R' = alkyl or aryl.[6] However, cations Fe(sb)₃²⁺ of this type of ligand introduce the possible complication of *mer* and *fac* isomers; isomer mixtures or isomerization may well interfere with substitution kinetic studies (cf. racemization in parallel with substitution at optically active complexes of the Fe(phen)₃²⁺ type[7]). The problem of isomeric forms may be avoided by the use of symmetrical diimines, **4**,[8] derived from α-diketones such as glyoxal (R = H) and biacetyl (butane-2,3-dione; R = CH₃), which have long been known to form very stable, intensely colored, iron(II) complexes.[9-11] Indeed,

* Author to whom correspondence should be addressed.
† University of Leicester.
‡ On leave from the Departamento de Quimica Fisica, Universidad de Sevilla, Sevilla, Spain.
§ University of New Hampshire.

(1) Parker, A. J. *Chem. Rev.* **1969**, *69*, 1.
(2) Blandamer, M. J.; Burgess, J. *Pure Appl. Chem.* **1979**, *51*, 2087; *Coord. Chem. Rev.* **1980**, *31*, 93; *Pure Appl. Chem.* **1982**, *54*, 2285; **1983**, *55*, 55.
(3) van Eldik, R. In *Inorganic High Pressure Chemistry-Kinetics and Mechanisms*; van Eldik, R., Ed.; Elsevier: Amsterdam, 1986; Section 1.5. Isaacs, N. S. *Liquid Phase High Pressure Chemistry*; Wiley: New York, 1981; Chapter 4.
(4) Lee, T. S.; Kolthoff, I. M.; Leussing, D. L. *J. Am. Chem. Soc.* **1948**, *70*, 2348, 3596. Krumholz, P. *Nature (London)* **1949**, *163*, 724. Baxendale, J. H.; George, P. *Ibid.* **1949**, *163*, 725; *Trans. Faraday Soc.* **1950**, *46*, 736. Basolo, F.; Hayes, J. C.; Neumann, H. M. *J. Am. Chem. Soc.* **1954**, *76*, 3807. Krumholz, P. *J. Phys. Chem.* **1956**, *60*, 87. Dickens, J. F.; Basolo, F.; Neumann, H. M. *J. Am. Chem. Soc.* **1957**, *79*, 1286.
(5) Burgess, J.; Pelizzetti, E. *Gazz. Chim. Ital.* **1988**, *118*, 803.
(6) Bähr, G.; Thämlitz, H. *Z. Anorg. Allg. Chem.* **1955**, *282*, 3. Bähr, G.; Döge, H.-G. *Ibid.* **1957**, *292*, 119.
(7) Yamagishi, A. *Inorg. Chem.* **1986**, *25*, 55.
(8) Pechmann, H. V. *Chem. Ber.* **1888**, *21*, 1412.